Available online at www.sciencedirect.com

ScienceDirect

journal homepage: www.elsevier.com/locate/burns

Bioactive peptide amphiphile nanofiber gels enhance burn wound healing

Situo Zhou [a,b,1], Akishige Hokugo [a,1], Mark McClendon [c], Zheyu Zhang [a], Reena Bakshi [a], Lixin Wang [a,d], Luis Andres Segovia [a], Kameron Rezzadeh [a], Samuel I. Stupp [c,e,f,g,h], Reza Jarrahy [a,*]

[a] Regenerative Bioengineering and Repair (REBAR) Laboratory, Division of Plastic and Reconstructive Surgery, Department of Surgery, David Geffen School of Medicine, University of California Los Angeles, Los Angeles, CA, USA
[b] Department of Burns and Reconstructive Surgery, Xiangya Hospital, Central South University, Changsha, Hunan, China
[c] Simpson Querrey Institute , Northwestern University, Chicago, IL, USA
[d] Department of Dentistry, Chengdu Women and Children's Central Hospital, Chengdu, Sichuan, China
[e] Department of Materials Science and Engineering, Northwestern University, Evanston, IL, USA
[f] Department of Chemistry, Northwestern University, Evanston, IL, USA
[g] Department of Medicine, Northwestern University, Chicago, IL, USA
[h] Department of Biomedical Engineering, Northwestern University, Evanston, IL, USA

ARTICLE INFO

Article history:
Accepted 16 June 2018

Keywords:
Self-assembly
Peptide amphiphile
Nanofiber
Thermally damaged cells
Wound healing

ABSTRACT

Background: Burns are physically debilitating and potentially fatal injuries. The standard-of-care for burn wounds is the coverage with gauze dressings designed to minimize trauma to the regenerating epidermis and dermis during dressing changes. However, deep partial- and full-thickness burns always heal slowly when standard wound care alone is performed. We have previously reported that peptide amphiphile (PA) gels, pH-induced self-assembling nanostructured fibrous scaffolds, promote cell proliferation and have great potential in regenerative medicine for rapid repair of tissues. In this study, we hypothesized that the PA gels are capable of accelerating wound healing in burn injury.

Methods: Artificially generated thermally damaged fibroblasts and human umbilical vein endothelial cells were seeded onto the various PA nanofiber gels including bioactive and nonbioactive peptide sequences. Cell proliferation was assessed at different time points, and thermally damaged fibroblasts and HUVECs manifested increased proliferation with time when cultured with various PA gels. To determine *in vivo* effects, burn wounds of rats were treated with the bioactive Arg-Gly-Asp-Ser (RGDS)-modified gel that showed greater cell proliferation *in vitro*. The wound closure was observed, and skin samples were harvested for histologic evaluation.

Results: Cell proliferation using the RGDS-PA gel was significantly higher than that observed in other gels. The RGDS-PA gel significantly enhanced re-epithelialization during the burn wound healing process between days 7 and 28. Application of PA gels accelerates the recovery

* *Corresponding author at*: Division of Plastic and Reconstructive Surgery, Department of Surgery, David Geffen School of Medicine at UCLA, 200 UCLA Medical Plaza, Suite 465 Los Angeles, CA 90095-6960, USA.
E-mail address: rjarrahy@mednet.ucla.edu (R. Jarrahy).
[1] These authors contributed equally to this study.
https://doi.org/10.1016/j.burns.2018.06.008

of deep partial-thickness burn wounds by stimulation of fibroblasts and the creation of an environment conducive to epithelial cell proliferation and wound closure.
Conclusions: This biomaterial represents a new therapeutic strategy to overcome current clinical challenges in the treatment of injuries resulting from burns.

1. Introduction

A significant number of burn injuries occur in the United States with more than 2.5 million Americans suffering with the sequelae of these wounds [1]. While the advances in burn management and care have improved leading to increased survival, there are a greater portion of patients remaining to combat the often-severe morbidities of long-term functional and esthetic deficits. The majority of these deficits are secondary to hypertrophic scarring for which there is no great preventive therapy [2]. Current wound management continues to rely on various topical agents and wound dressings, followed by autologous skin grafting and its associated morbidities of pain, infection, and scarring, as the current gold standard.

Denatured dermis plays an essential role in wound healing, and preservation of denatured dermis may be an effective treatment for skin burns to attenuate scar formation and restore normal appearance [3]. It is well known that the dermis predominantly comprises fibroblasts and vascular endothelial cells [4]. These cells must be bound up in the recovery of the thermally damaged dermis. In fact, therapies designed to support and augment the regenerative capacity of these cells have demonstrated to lessen scar contracture and, ultimately, to improve appearance and function [5,6].

Peptide amphiphile (PA) nanofiber hydrogels have been shown to direct cell fate through both physical and molecular signaling [7,8]. Interestingly, these PA gels can not only maintain a hydrated scaffold to support cell growth but also have the ability to display important bioactive peptide sequences that mimic native tissues such as collagen or laminin [9,10]. The constituent PA molecules making up the nanofibers consist of four main segments: (1) a hydrophobic group (2) a β-sheet-forming peptide that promotes nanofiber formation; (3) a peptide segment that contains ionizable side chain residues for solubility; and (4) an optional bioactive signaling epitope designed to interact with cellular receptors and stimulate cellular activities (Fig. 1). The RGDS (Arg-Gly-Asp-Ser) epitope sequence is found naturally on molecules of fibronectin and has been shown to promote cellular motility, proliferation, and differentiation in vitro [11–15]. It has been used in a variety of cells types including osteoblasts [16], Schwann cells [17], and neurons [18]. The use of the RGDS in self-assembled structures and their influence on cellular behavior has been investigated for cell adhesion, cell delivery, differentiation, and morphology [9,19–21].

The purpose of this study is to investigate a novel bioactive nanofiber-based hydrogel biomaterial that can accelerate burn wound healing. To achieve this purpose, various hydrogels were applied to the thermally damaged cells to identify the appropriate bioactive nanofiber hydrogel. Moreover, *in vivo* studies were performed to investigate the use of the appropriate bioactive nanofibers as a wound dressing in a rat burn model and subsequently examined in the context of burn wound healing.

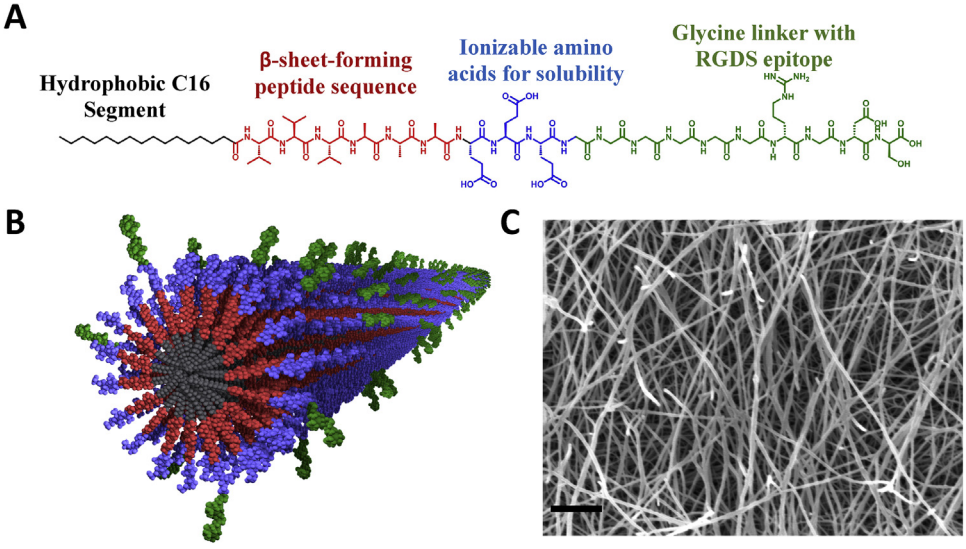

Fig. 1 – A: Chemical structure of the bioactive PA molecule used in the PA5 group. B: The colored segments correspond to the 3D illustration of a nanofiber composed of 10% bioactive PA molecules. These nanofibers readily form gels through ionic crosslinks. C: The gel is viewed in SEM as an interconnected network of fibers. Scale bar: 500 nm.

2. Materials and methods

2.1. Cell cultures and establishment of thermally damaged cell models

Normal human fibroblasts (hFBs) (CCD-1127Sk) and human umbilical vein endothelial cells (HUVECs) were obtained from American Type Culture Collection (ATCC) (Manassas, VA, USA). The hFBs were maintained in Dulbecco's Modified Eagle Medium (DMEM) (Corning Inc., Corning, NY, USA) with 10% fetal bovine serum (FBS) (Life Technologies, Carlsbad, CA, USA) and penicillin/streptomycin (Life Technologies, Carlsbad, CA, USA). The HUVECs were cultured in EGM-2 medium with endothelial cell growth supplement (SingleQuots, LONZA, Basel, Switzerland). The medium was changed every 72 h. All cell cultures were maintained at 37 °C and 5% CO_2. When hFBs and HUVECs reached to 80% confluence, cells were harvested with 0.25% trypsin-EDTA (Life Technologies, Carlsbad, CA, USA) and resuspended in phosphate-buffered saline (PBS) with cell density of 1×10^5 cells/ml into sterile microcentrifuge tubes (Thermo Fisher Scientific, Waltham, MA, USA). Each tube contained 2 ml of cell suspension. Microcentrifuge tubes containing the cells were immersed in the water bath at various temperatures: 37 °C, 52 °C, and 100 °C for 90 s. After immersion, cells were resuspended in fresh medium and seeded in 96-well plates with 1×10^4 cells per well for 6 h.

2.2. Cell damage assay

HCS DNA damage kit (Invitrogen, Carlsbad, CA, USA) was used to evaluate cell damage in terms of genotoxicity and cytotoxicity according to the manufacturer's protocol. Briefly, cells were washed twice with PBS before fixing with 4% paraformaldehyde. After washing with PBS, cells were stained with phosphorylated H2AX and Image-iT® DEAD Green™ and then photographed using a fluorescence imaging microscope (Leica DMI6000 B, Leica Microsystems Inc., Wetzlar, Germany). The fluorescence intensities for each staining were analyzed with a microplate reader (Synergy H1 Multi-mode Reader, BioTek, Winooski, VT, USA).

2.3. Synthesis of various PA hydrogels

All PAs were synthesized in the Simpson Querrey Institute's Peptide Synthesis Core at Northwestern University. PA synthesis was carried out using an automated peptide synthesizer (CEM Liberty microwave-assisted, CEM Corporation, Matthews, NC, USA) by standard 9-fluorenyl methoxycarbonyl (Fmoc) solid-phase peptide synthesis on rink amide MBHA resin or Glu (OtBu) Wang resin (Sigma-Aldrich, St. Louis, MO, USA). PAs were purified by reverse-phase HPLC (Varian ProStar 210 HPLC, Varian, Inc., Palo Alto, CA, USA) using a water/acetonitrile (each containing 0.1% v/v ammonium hydroxide) gradient. Eluting fractions containing the desired PA were confirmed by mass spectrometry (Agilent 6520 LCMS, Agilent Technologies, Santa Clara, CA, USA). Confirmed fractions were pooled, and the acetonitrile was removed by rotary evaporation before freezing and lyophilization. The purity of lyophilized products was tested by LCMS (Agilent 6520 LCMS, Agilent Technologies, Santa Clara, CA, USA). After lyophilization, PAs were dissolved at ~1% w/v in mQ water, and the pH was adjusted to ~7 with NaOH, making PAs completely soluble. These solutions were then dialyzed against mQ water and lyophilized again. These lyophilized PA powders were soluble when resuspended in water buffers (Fig. 1).

2.4. PA-cell gel fabrication

To prepare the PA gels, PAs were dissolved in aqueous 150 mM NaCl, 3 mM KCl, and NaOH solution to obtain a final 1 wt% solution at a pH between 7.2 and 7.4. To fabricate mixtures containing epitope-bearing PAs, the backbone-PA (PA1 or PA4) was dissolved in aqueous 150 mM NaCl, 3 mM KCl, and NaOH solution to obtain a 1.33 wt% solution at a pH between 7.2 and 7.4. The epitope-containing PA (PA3 or PA5) was then dissolved with the same solution to obtain a 1 wt% solution at a pH between 7.2 and 7.4. The 1.33 wt% PA solution was then mixed in a 3:1 ratio with the 1% bioactive epitope solution creating a final bioactive-PA solution of 1.25 wt%, 1 wt% base sequence (PA1 or PA4), and 0.25 wt% bioactive PA (PA3 or PA5). The resulting solutions were then heated to 80 °C for 30 min in a water bath and left in the bath for slow cooling to 23 °C overnight [8,22]. Table 1 describes the PA groups tested in these experiments.

Following completion of the slow cooling, each of the PA solutions was mixed with thermally damaged (52 °C for 90 s) hFB or HUVEC suspensions in a 4:1 ratio. The final cell density was 3500 cells/μl. The solutions were pipetted in 96-well culture plates, and 15 mM CaCl2 was added for 1 h. Solutions were then gelled by calcium ions. The thermally damaged cells were seeded onto the gels with 1000 cells per well.

To prepare the control group, volumetric ratios of 1 μl HEPES, 10 μl 10X PBS, 87 μl of collagen 10 mg/ml, and thermally damaged hFB or HUVEC PBS suspension were combined and gently mixed to give a final cell density of 3500 cells/μl. We

Table 1 – Design of various PA.

PA group	Amino acid sequence	Termination	Bioactive sequence
PA1	C16-VVAAEE	$-NH_2$	N/A
PA2	C16-VVAAEE	–COOH	N/A
PA3*	C16-VVAAEERGDS	$-NH_2$	RGDS
PA4	C16-VVVAAAEEE	$-NH_2$	N/A
PA5**	C16-VVVAAAEEEGGGGGRGDS	$-NH_2$	RGDS

* and ** designate the PA was mixed at a 9:1 molecular ratio with its backbone sequence of PA2 and PA4, respectively.

then pipetted the mixture into a 94-well culture plate well and allowed the solution to cure and solidify for 1 h at 37 °C prior to the addition of cell medium [23]. For a second control group, cells were simply seeded at 1000 cells per well.

2.5. Cell proliferation assay

To evaluate the viability of cells within the gels, WST-1 reagent (Roche Applied Science, Indianapolis, IN, USA) was used for each PA-cell and collagen gel–cell complex. Following each time point (1, 2, 3, and 5 days), gel complexes were incubated for 4 h in 100 μl of cell culture medium containing 10% WST-1 assay reagent, and absorption values were read in a spectrophotometer at 450 nm. Measurements were repeated three times.

2.6. Rat burn model and treatment

Animal procedures and protocols were reviewed and approved by the Animal Research Committee of the University of California Los Angeles. Sprague Dawley rats (average weight: 300 g) were purchased from Charles River Laboratories (Wilmington, MA, USA) and were housed and maintained at the UCLA vivarium under the care of the veterinary staff, according to the regulations set forth by the UCLA Office of Protection of Research Subjects. A deep partial-thickness burn model was artificially manufactured according to the established procedure with modification [24]. Briefly, animals were anesthetized with inhalational anesthetic of 2.5% isoflurane and their dorsal hair clipped. A stainless steel cylinder (1.76 cm in diameter, 1.78 cm in height) was heated to 100 °C in a water bath for 10 min and placed on the back of rats for 10 s to cause deep partial-thickness burn wound. Pathological examination confirmed this, and the burns penetrated to the dermal skin layer. Pathological examination at day 1 after the burn confirmed that the burns penetrated to the dermal skin layer. Intact dermis was observed while most of dermis and epidermis were destructed with the thin crust (Supplemental Fig. 1). To elucidate the availability of bioactive epitopes of PA nanofiber gels, 150 μl of PA4 or PA5, which covered the entire wound and the surrounding area, was applied on the wound without excision (n = 6 each). The control group (n = 6) received no treatment. Tegaderm™ (3M, St. Paul, MN, USA) and VetrapTM Bandaging tape (3M, St. Paul, MN, USA) were used to protect the wounds. The animals were euthanized using carbon dioxide followed by decapitation and skin specimens were harvested at days 7 and 28 after burn, respectively. The normal skin specimens were also collected from the back of rats.

2.7. Histological examination

The skin specimens were fixed in 4% formaldehyde for 48 h, embedded in paraffin, and cut into 4 mm sections. Slides were stained with hematoxylin and eosin (H&E) and observed under a microscope (Olympus BX51, Olympus, Tokyo, Japan). Wound re-epithelialization was measured by planimetry using ImageJ software (National Institutes of Health, Bethesda, MD, USA). The results are expressed as the percentage of wound area that had re-epithelialized. Moreover, the numbers of capillaries were counted manually in the burn area at ×200 magnification in each section. Histological sections were also stained with picrosirius red (Picrosirius Red Stain Kit, Polysciences, Warrington, PA, USA) according to the manufacturer's protocol and observed under a microscope with circularly polarized light (Olympus BX43, Olympus, Tokyo, Japan) at ×200 magnification to analyze the collagen deposition after burn injury [25].

2.8. Statistical analysis

One-way analysis of variance (ANOVA) was performed for comparing groups. The Tukey–Kramer multicomparison adjustment was used as the post-hoc test to calculate the significance levels. $P < 0.05$ was considered as statistically significant.

3. Results

3.1. Establishment of thermally damage cell models

The hFB and HUVECs were treated at various temperatures (37, 52, and 100 °C) for 90 s. DNA damage was measured as an indication of genotoxicity and accomplished by specific antibody-based detection of phosphorylated H2AX in the nucleus. Thermal damage leading to serious cell injuries, including plasma membrane permeability, was measured using Image-iT® DEAD GreenTM viability. The number of hFB and HUVECs treated at 52 °C exhibited a significant decrease in DAPI expression compared to cells treated at 37 °C. Approximately 50% of hFBs and HUVECs treated with 52 °C expressed red and green fluorescence that represented genotoxicity and cytotoxicity, respectively (Fig. 2A and B, lower graphs). All cells treated with 100 °C showed red and green fluorescence intensities. This indicates that all cells were completely dead.

3.2. Proliferation of thermally damaged cells in PA or collagen gels

Thermally damaged hFBs (Fig. 3A) and HUVECs (Fig. 3B) manifested increased proliferation with time when cultured with various PA and collagen gels. Viability measurements at day 3 demonstrated that cells proliferated more rapidly in PA5 gels than in other gels. On day 5, proliferation of hFB and HUVECs in both PA3 and PA5 was significantly higher than that of hFB and HUVECs in backbone-PA (PA2 and PA4, respectively) in the collagen gel alone. Overall, proliferation in PA5 was the highest among all groups and was thus used for the following *in vivo* experiment. PA4, the backbone PA of PA-5, was also tested to determine the *in vivo* effects of the bioepitope on wound healing.

3.3. Burn wound healing in rats with PA gel

To determine the effect of PA gel on the recovery of burns on rats, the wounds were visually monitored and photographed. On day 0, all burn wounds were waxy white with surrounding erythema. By day 7, all wounds showed eschar formation. After day 14, wound healing was accelerated with application of PA5 gel compared to other groups. The wound area and the

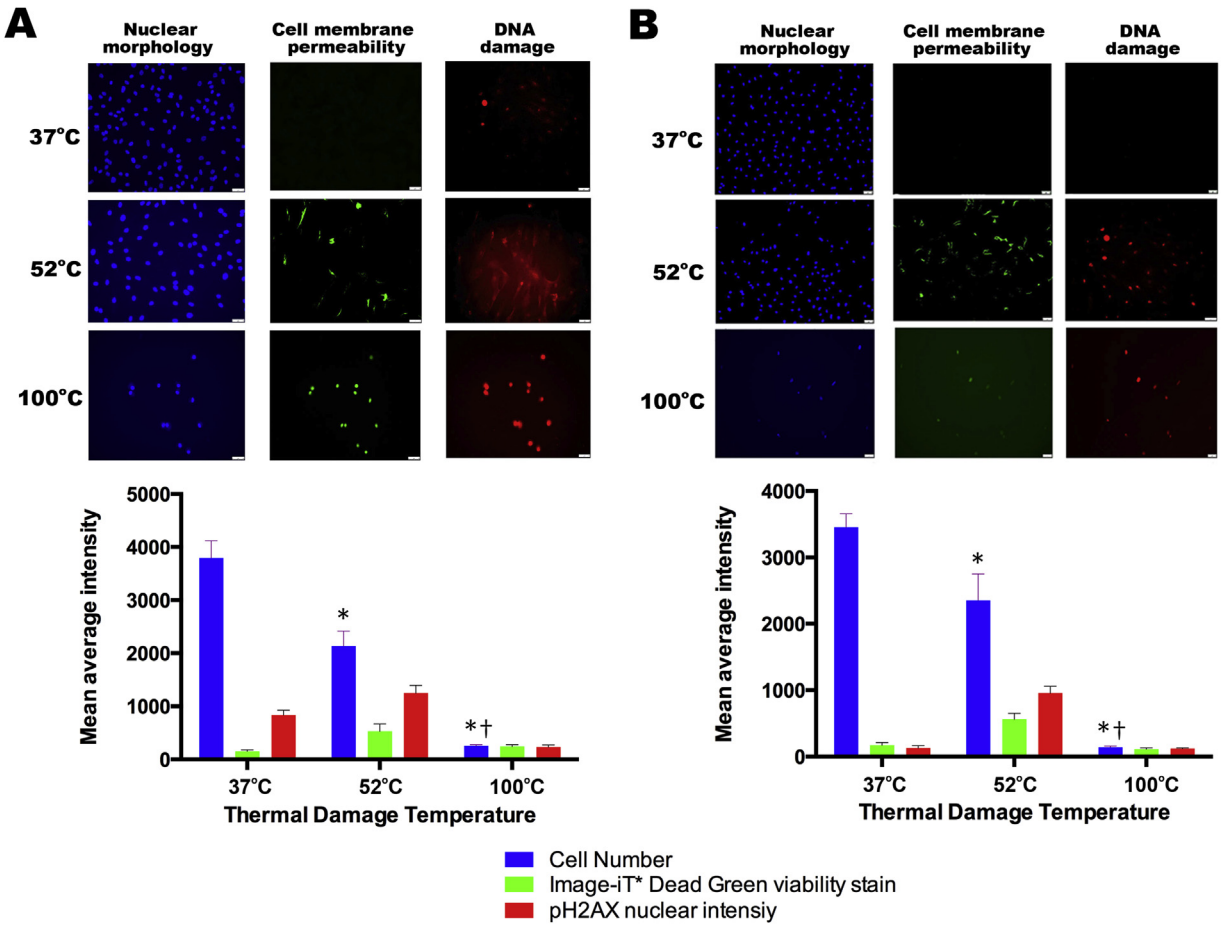

Fig. 2 – Microscopic images of genotoxicity and cytotoxicity of thermally damaged hFBs (A) and HUVECs (B) by using the HCS DNA Damage Kit. The cells were treated at 37, 52, and 100 °C for 90 s. At 52 °C, approximately 50% cells were positive for pH2AX indicating DNA damage, and Image-iT® DEAD Green™ viability stain defining compromise in plasma membrane integrity. At 100 °C, cells showed nearly 100% genotoxic and cytotoxic effects as demonstrated by the positive pH2AX and Image-iT® DEAD Green™ viability stain fluorescence. Hoechst 33342 was used as a nuclear segmentation dye. The graphs represent quantitative representation of quantitative fluorescence intensities. Data are represented as mean ± SD of six determinations. * $p \leq 0.05$ against the value of 37 °C, † $p \leq 0.05$ against the value of 52 °C.

percentage of re-epithelialization were quantitatively assessed to evaluate the rate of healing by planimetry. The application of PA5 gel significantly enhanced wound closure and re-epithelialization during burn wound healing process (Fig. 4). Wounds treated with PA4 and PA5 gels were observed to evaluate the effect of bioactive epitopes of PA nanofiber gels on recovery of burns. Our results demonstrated a representative photomicrograph of HE-stained skin sections from PA4, PA5, and control groups (Fig. 5). At day 7, all groups showed complete destruction of dermis and epidermis with epidermal detachment, edema, and crust formation of necrotic tissue remnants. The PA5-treated wound showed less edema and increased fibroblast infiltration compared with other groups. On day 28, wound healing was accelerated on treatment with the PA5 gel compared to other groups (Fig. 5). Significant stimulatory effects were observed on granulation with fibroblast infiltration and capillary formation in PA5 gel-treated wounds. The number of capillaries in the PA5-treated wound was significantly higher than those of PA4-treated ($P \leq 0.001$) and control ($P \leq 0.0001$) wounds (Fig. 6A). Furthermore, the application of PA5 gel significantly enhanced wound closure and re-epithelialization during the burn wound healing process between days 7 and 28 compared with the control wound ($P \leq 0.05$) (Fig. 6B). Thicker collagen fibers were aligned in PA5 gel-treated wounds than the collagen fibers in the PA4-treated wound (Fig. 6C).

4. Discussion

Regeneration of the epidermis, neovascularization, and proliferation of fibroblasts are necessary processes during burn wound healing. [26]. Creating an ideal environment for these to occur in the absence of infection while maintaining hydration is a key aspect of treatment. For bring that effect, various hydrogels are used as wound dressings [27,28]. Herein, we use a hydrogel capable of assembly into nanofibers, with specific binding properties through an RGDS epitope [29,30].

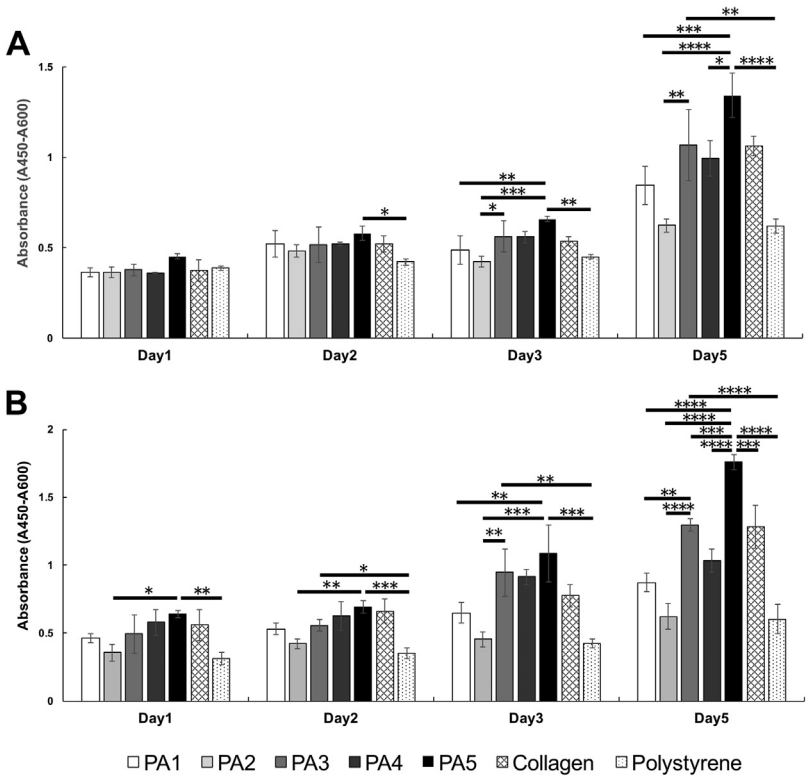

Fig. 3 – hFB (A) and HUVEC (B) proliferation in various gels. RGDS-PAs statistically increased cell proliferation against backbone PA at Day 5. All p values were calculated using ANOVA and the Tukey-Kramer test. * $P \leq 0.05$, ** $P \leq 0.01$, *** $P \leq 0.001$, and **** $P \leq 0.0001$. Statistically significant differences related to PA3 or PA5 are represented in the graph as asterisks.

The RGDS epitope is a well-recognized sequence within the ECM and plays a role in cell recruitment [31]. Our previous work has demonstrated the ability of these PA gels to provide an environment that promotes tissue regeneration in a peripheral nerve injury model [17]. Using the results from this work, we believe that providing a suitable microenvironment by native cell recruitment will aid in intrinsic regeneration of burn wounds, thus leading to accelerated and superior wound healing.

After the immediate inflammatory response to burn injuries, the infiltration of the wound site by fibroblasts and other cell types initiates the proliferative phase [32]. The function of fibroblasts is primarily collagen deposition in the dermal wound area [33,34]. Increased production of type III

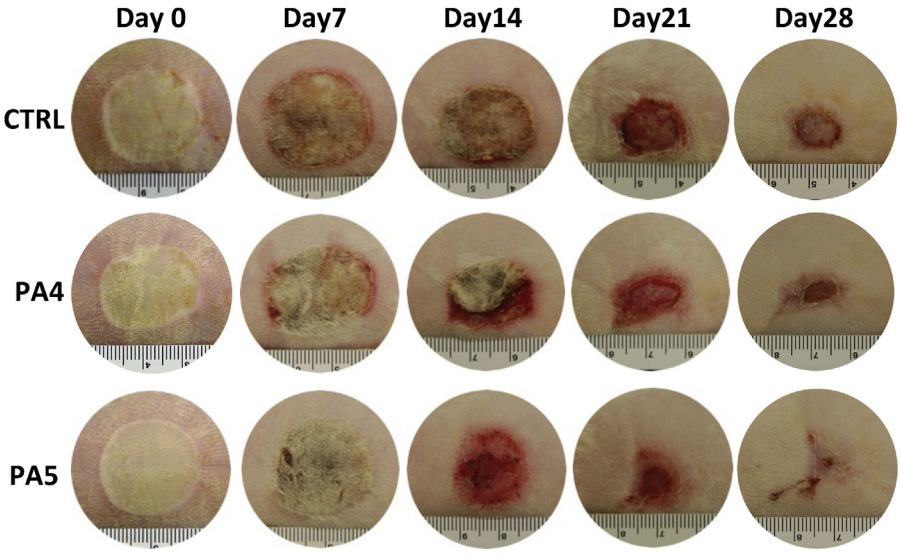

Fig. 4 – Gross observation of burn wound healing treated with PA4, PA5, or no treatment (CTRL).

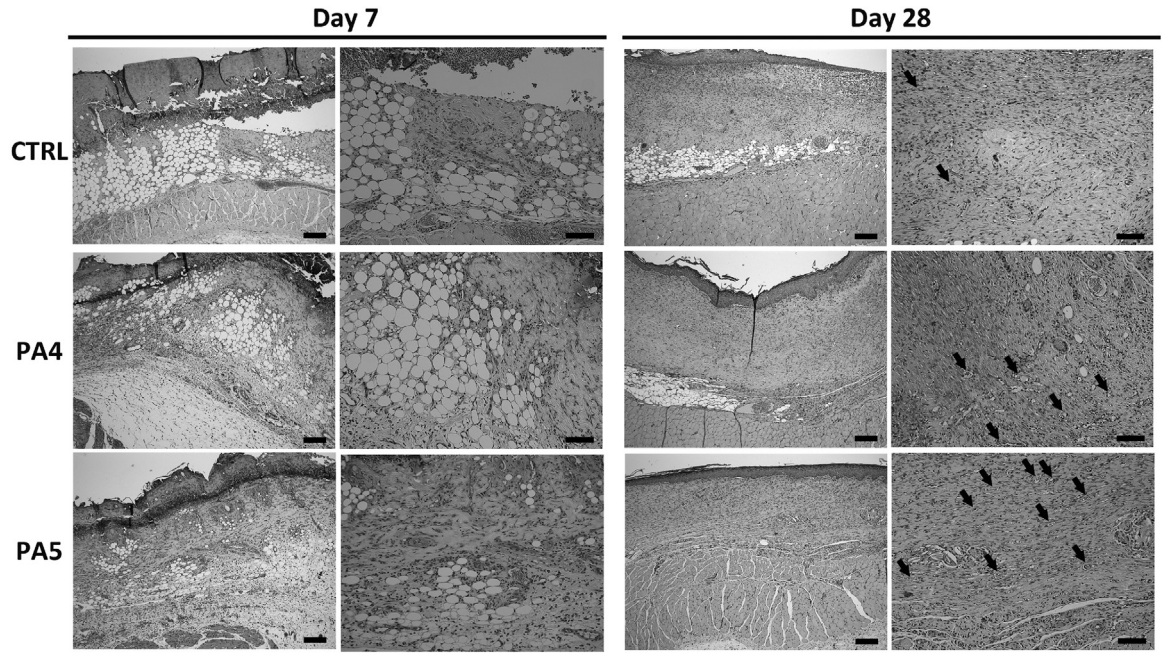

Fig. 5 – Histological findings at days 7 and 28. The transverse section of the PA5 group compared with those of the PA4 and control (CTRL) groups are visualized by H.E. staining. Black arrows represent capillaries.

collagen and fibronectin occurs within the first 3 days after tissue injury [35]. This activates several signaling pathways that modulate healing [36]. Fibroblasts also secrete cytokines that attract keratinocytes to the injury [37], which function in re-epithelialization of the wound site and ultimately restoration of the barrier function of epithelium [33,34]. Angiogenesis occurs concurrently with fibroblast and keratinocyte proliferation and migration. This is critical for wound healing because

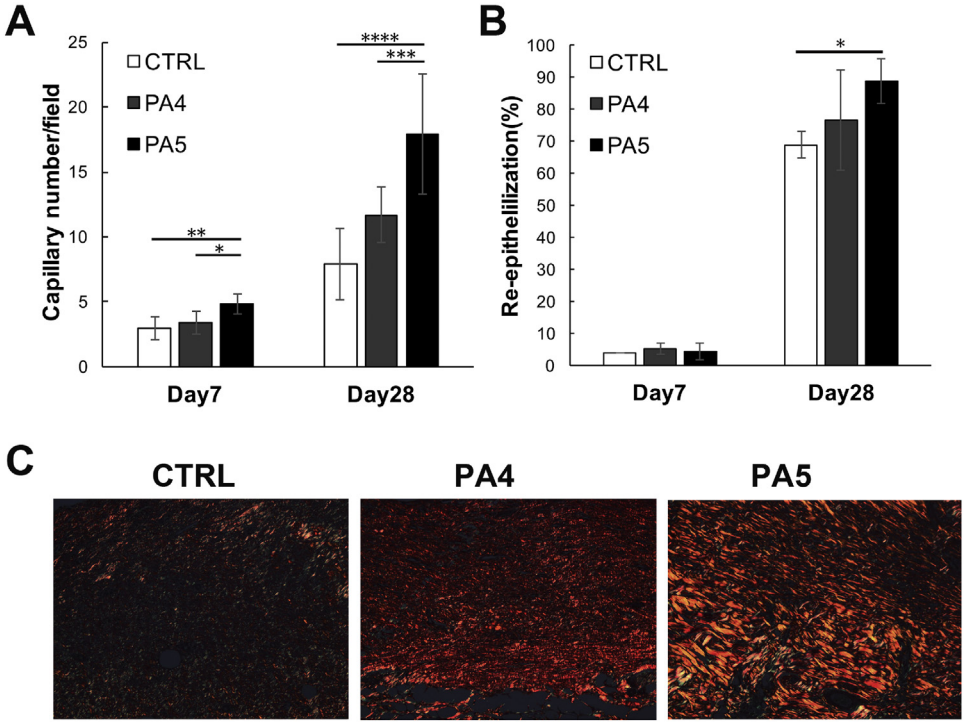

Fig. 6 – (A) Stimulation of capillary formation on days 7 and 28 in the PA4, PA5, and control (CTRL) groups. The number of capillary lumens per microphotographic field was counted. (B) Quantitative evaluation of PA4- and PA5-treated wound healing and untreated wound healing (CTRL) by planimetry. The error bars denote mean ± SD. * $P \leq 0.05$, ** $P \leq 0.01$, *** $P \leq 0.001$, and **** $P \leq 0.0001$. (C) Observation of collagen fibrils by picrosirius red staining with polarized light. Collagen I appear red (×200). (For interpretation of the references to color in this figure legend, the reader is referred to the web version of this article.)

fibroblasts and epithelial cells require a continuous supply of oxygen and nutrients for optimal function and cell division [34]. Angiogenesis results from the sprouting of new capillaries from existing vessels [38] by endothelial cell activation, proliferation, and migration to form new vessels [39]. Enhancing angiogenesis in addition to the proliferation and migration of fibroblasts would accelerate wound healing following burns. Several groups have examined factors leading to the acceleration of wound healing *in vivo*; however, a paucity of data exists on the behavior of thermally damaged HUVECs *in vitro* [24,40]. In the present study, we assessed the morphological character of fibroblasts and HUVECs after heat injury. Liang and Jiang et al. established the thermally damaged fibroblast and HUVEC model at 52°C for 30s [4,40]. On the basis of this notion, our study involved different durations (30s, 60s, 90s, and 180s) at 52°C for fibroblasts and HUVECs (data not shown). The experiments showed that half of the cells underwent genotoxic and cytotoxic effects at 52°C for 90s, which most likely reflect the physiological characteristics of cells in deep second-degree burn injury [41].

Our previous work with PA gels alerted us to the fact that the stiffness of the nanofiber scaffold derived from these gels may negatively impact their ability to interact with cells; this mechanical property was mitigated by the addition of modified amino acid sequences [42,43]. In this study, we examined C16-V2A2E2 and C16-V3A3E3, which comprise a hydrophobic alkyl tail that is covalently conjugated to a variable number and position of peptide segment composed of valine (V), alanine (A), and glutamic acid (E). Surprisingly, the results demonstrated that the use of both C16-V2A2E2-NH2-RGDS (PA3) and C16-V3A3E3-NH2-RGDS (PA5) gels significantly increased the proliferation of thermally damaged fibroblasts and HUVECs compared to the backbone PA gel. In particular, the PA5 gel showed the highest proliferation in both thermally damaged fibroblasts and HUVECs, a result consistent with the fibronectin-like conformation of the RGDS epitope and its physiological role as discussed above.

Various animal models for burns are used to study burn injury. These models should be standardized to obtain injuries with the same size and depth degree. We used a rat model owing to easy handling, accommodation, and low mortality. In our rat burn injury model, the burn wound had waxy white color with peripheral erythema that was mild and no blisters. These appearances are similar to the definition of deep partial-thickness burns [44]. To generate deep partial-thickness burns, Tavares Pereira Ddos et al. [45] positioned a massive aluminum bar, which was preheated to 99°C±2°C for 10min on the back of each animal for 15s. They confirmed the acquisition of deep second-degree burns based on the observation of total autolysis of both the dermis and epidermis without reaching the hypodermis. Akhoondinasab et al. [46] also created a deep second-degree burn wound with a hot plate heated with boiling water and placed for 10s on the skin with an equal pressure over the lower back, and a third-degree burn with 30s of pressure was made over the upper back. According to these studies, direct contact with a heated solid is ideal to generate deep partial-thickness burns and is suitable for the investigation of the efficacy of PA gels.

The results of *in vivo* studies further support the value of applying the RGDS-PA scaffold to the burn injury. PA gels can penetrate into the skin through the surrounding healthy area rather than the wound itself and provide a nurturing microenvironment for tissue repair within the healing area. PA nanofibers would need to penetrate through the skin barrier. The stratum corneum, which is a key feature of this barricade and a layer of tightly packed keratinized dead cells, forms the outermost component of the epidermis. The only ingress across this layer is through nanopore lacunae between the corneocytes. The average thickness of the extracellular space between the corneocytes is 44nm [47]. The PA nanofibers are ~10nm in diameter [8]. During the healing process, the nanofibers form their penetrating tracts through slightly damaged extracellular spaces in the skin even though there is no driving force to penetrate the skin. Wound closure was significantly faster for injuries treated with PA gel than the control. The regeneration of the epidermis was almost complete for PA gel-treated wounds. Re-epithelialization of 80.5% was achieved, which was remarkably higher than the 42.3% for non-PA-treated wounds. Furthermore, histological analysis of the burn wound sites is consistent with our *in vivo* findings. The PA-treated wounds exhibited better granulation tissue and capillary formation than the control wounds at days 7 and 28. These data support the ability of PA gels to induce migration and proliferation of epithelial cells and fibroblasts to accelerate wound healing.

5. Conclusions

The application of PA gels accelerates the recovery of deep partial-thickness burn wounds by stimulation of fibroblast and epithelial cell proliferation, thus promoting burn wound closure. We believe that this biomaterial represents a new therapeutic strategy to overcome challenges we currently face in treating clinical burn injuries.

Acknowledgments

This work was supported by the Annenberg Fund for Craniofacial Surgery and Research at UCLA. S.I.S. research was supported by the Northwestern University Center for Regenerative Nanomedicine through a CRN Catalyst Award.

Conflicts of interest

None.

Appendix A. Supplementary data

Supplementary data associated with this article can be found, in the online version, at https://doi.org/10.1016/j.burns.2018.06.008.

REFERENCES

[1] Soto-Pantoja DR, Shih HB, Maxhimer JB, Cook KL, Ghosh A, Isenberg JS, et al. Thrombospondin-1 and CD47 signaling regulate healing of thermal injury in mice. Matrix Biol 2014;37:25–34.

[2] Akershoek JJ, Vlig M, Talhout W, Boekema BK, Richters CD, Beelen RH, et al. Cell therapy for full-thickness wounds: are fetal dermal cells a potential source? Cell Tissue Res 2016;364:83–94.
[3] Zhang X, Yang J, Zhao J, Zhang P, Huang X. MicroRNA-23b inhibits the proliferation and migration of heat-denatured fibroblasts by targeting Smad3. PLoS One 2015;10:e0131867.
[4] Jiang B, Li Y, Liang P, Liu Y, Huang X, Tong Z, et al. Nucleolin enhances the proliferation and migration of heat-denatured human dermal fibroblasts. Wound Repair Regen 2015;23:807–18.
[5] Papini R. Management of burn injuries of various depths. BMJ 2004;329:158–60.
[6] Liang P, Lv C, Jiang B, Long X, Zhang P, Zhang M, et al. MicroRNA profiling in denatured dermis of deep burn patients. Burns 2012;38:534–40.
[7] Webber MJ, Tongers J, Newcomb CJ, Marquardt KT, Bauersachs J, Losordo DW, et al. Supramolecular nanostructures that mimic VEGF as a strategy for ischemic tissue repair. Proc Natl Acad Sci U S A 2011;108:13438–43.
[8] Zhang S, Greenfield MA, Mata A, Palmer LC, Bitton R, Mantei JR, et al. A self-assembly pathway to aligned monodomain gels. Nat Mater 2010;9:594–601.
[9] Guler MO, Hsu L, Soukasene S, Harrington DA, Hulvat JF, Stupp SI. Presentation of RGDS epitopes on self-assembled nanofibers of branched peptide amphiphiles. Biomacromolecules 2006;7:1855–63.
[10] Sur S, Guler MO, Webber MJ, Pashuck ET, Ito M, Stupp SI, et al. Synergistic regulation of cerebellar Purkinje neuron development by laminin epitopes and collagen on an artificial hybrid matrix construct. Biomater Sci 2014;2:903–14.
[11] Houseman BT, Mrksich M. The microenvironment of immobilized Arg-Gly-Asp peptides is an important determinant of cell adhesion. Biomaterials 2001;22:943–55.
[12] Irvine DJ, Mayes AM, Griffith LG. Nanoscale clustering of RGD peptides at surfaces using Comb polymers. 1. Synthesis and characterization of Comb thin films. Biomacromolecules 2001;2:85–94.
[13] Irvine DJ, Ruzette AV, Mayes AM, Griffith LG. Nanoscale clustering of RGD peptides at surfaces using comb polymers. 2. Surface segregation of comb polymers in polylactide. Biomacromolecules 2001;2:545–56.
[14] Jensen TW, Hu BH, Delatore SM, Garcia AS, Messersmith PB, Miller WM. Lipopeptides incorporated into supported phospholipid monolayers have high specific activity at low incorporation levels. J Am Chem Soc 2004;126:15223–30.
[15] Maheshwari G, Brown G, Lauffenburger DA, Wells A, Griffith LG. Cell adhesion and motility depend on nanoscale RGD clustering. J Cell Sci 2000;113(Pt 10):1677–86.
[16] Oh JH, Kim HJ, Kim TI, Baek JH, Ryoo HM, Woo KM. The effects of the modulation of the fibronectin-binding capacity of fibrin by thrombin on osteoblast differentiation. Biomaterials 2012;33:4089–99.
[17] Li A, Hokugo A, Yalom A, Berns EJ, Stephanopoulos N, McClendon MT, et al. A bioengineered peripheral nerve construct using aligned peptide amphiphile nanofibers. Biomaterials 2014;35:8780–90.
[18] Stephanopoulos N, Freeman R, North HA, Sur S, Jeong SJ, Tantakitti F, et al. Bioactive DNA- peptide nanotubes enhance the differentiation of neural stem cells into neurons. Nano Lett 2015;15:603–9.
[19] Storrie H, Guler MO, Abu-Amara SN, Volberg T, Rao M, Geiger B, et al. Supramolecular crafting of cell adhesion. Biomaterials 2007;28:4608–18.
[20] Huang Z, Sargeant TD, Hulvat JF, Mata A, Bringas Jr. P, Koh CY, et al. Bioactive nanofibers instruct cells to proliferate and differentiate during enamel regeneration. J Bone Miner Res 2008;23:1995–2006.
[21] Webber MJ, Tongers J, Renault MA, Roncalli JG, Losordo DW, Stupp SI. Development of bioactive peptide amphiphiles for therapeutic cell delivery. Acta Biomater 2010;6:3–11.
[22] Berns EJ, Sur S, Pan L, Goldberger JE, Suresh S, Zhang S, et al. Aligned neurite outgrowth and directed cell migration in self-assembled monodomain gels. Biomaterials 2014;35:185–95.
[23] Gabbay JS, Heller JB, Mitchell SA, Zuk PA, Spoon DB, Wasson KL, et al. Osteogenic potentiation of human adipose-derived stem cells in a 3-dimensional matrix. Ann Plast Surg 2006;57:89–93.
[24] Zhou S, Zhang P, Liang P, Huang X. The expression of miR-125b regulates angiogenesis during the recovery of heat-denatured HUVECs. Burns 2015;41:803–11.
[25] Velidandla S, Gaikwad P, Ealla KK, Bhorgonde KD, Hunsingi P, Kumar A. Histochemical analysis of polarizing colors of collagen using Picrosirius Red staining in oral submucous fibrosis. J Int Oral Health 2014;6:33–8.
[26] Alemdaroglu C, Degim Z, Celebi N, Zor F, Ozturk S, Erdogan D. An investigation on burn wound healing in rats with chitosan gel formulation containing epidermal growth factor. Burns 2006;32:319–27.
[27] Schneider A, Garlick JA, Egles C. Self-assembling peptide nanofiber scaffolds accelerate wound healing. PLoS One 2008;3:e1410.
[28] Philp D, Badamchian M, Scheremeta B, Nguyen M, Goldstein AL, Kleinman HK. Thymosin beta 4 and a synthetic peptide containing its actin-binding domain promote dermal wound repair in db/db diabetic mice and in aged mice. Wound Repair Regen 2003;11:19–24.
[29] Capito RM, Azevedo HS, Velichko YS, Mata A, Stupp SI. Self-assembly of large and small molecules into hierarchically ordered sacs and membranes. Science 2008;319:1812–6.
[30] Harrington DA, Cheng EY, Guler MO, Lee LK, Donovan JL, Claussen RC, et al. Branched peptide-amphiphiles as self-assembling coatings for tissue engineering scaffolds. J Biomed Mater Res A 2006;78:157–67.
[31] Hersel U, Dahmen C, Kessler H. RGD modified polymers: biomaterials for stimulated cell adhesion and beyond. Biomaterials 2003;24:4385–415.
[32] Amini-Nik S, Glancy D, Boimer C, Whetstone H, Keller C, Alman BA. Pax7 expressing cells contribute to dermal wound repair, regulating scar size through a beta-catenin mediated process. Stem Cells 2011;29:1371–9.
[33] Gurtner GC, Werner S, Barrandon Y, Longaker MT. Wound repair and regeneration. Nature 2008;453:314–21.
[34] Li J, Chen J, Kirsner R. Pathophysiology of acute wound healing. Clin Dermatol 2007;25:9–18.
[35] Stadelmann WK, Digenis AG, Tobin GR. Physiology and healing dynamics of chronic cutaneous wounds. Am J Surg 1998;176:26S–38S.
[36] Bielefeld KA, Amini-Nik S, Whetstone H, Poon R, Youn A, Wang J, et al. Fibronectin and beta- catenin act in a regulatory loop in dermal fibroblasts to modulate cutaneous healing. J Biol Chem 2011;286:27687–97.
[37] Alvarez OM, Kalinski C, Nusbaum J, Hernandez L, Pappous E, Kyriannis C, et al. Incorporating wound healing strategies to improve palliation (symptom management) in patients with chronic wounds. J Palliat Med 2007;10:1161–89.
[38] Isner JM, Asahara T. Angiogenesis and vasculogenesis as therapeutic strategies for postnatal neovascularization. J Clin Invest 1999;103:1231–6.
[39] Carmeliet P. Angiogenesis in life, disease and medicine. Nature 2005;438:932–6.
[40] Liang P, Jiang B, Lv C, Huang X, Sun L, Zhang P, et al. The expression and proangiogenic effect of nucleolin during the recovery of heat-denatured HUVECs. Biochim Biophys Acta 2013;1830:4500–12.
[41] Li D, Huang X, Yang X. Morphology of human skin fibroblasts after heat injury in vitro. J Clin Rehabil Tissue Eng Res 2008;12:2056–60.
[42] Pashuck ET, Cui HG, Stupp SI. Tuning supramolecular rigidity of peptide fibers through molecular structure. J Am Chem Soc 2010;132:6041–6.

[43] Greenfield MA, Hoffman JR, de la Cruz MO, Stupp SI. Tunable mechanics of peptide nanofiber gels. Langmuir 2010;26:3641–7.
[44] Johnson RM, Richard R. Partial-thickness burns: identification and management. Adv Skin Wound Care 2003;16:178–87 quiz 88-9.
[45] Tavares Pereira Ddos S, Lima-Ribeiro MH, de Pontes-Filho NT, Carneiro-Leao AM, Correia MT. Development of animal model for studying deep second-degree thermal burns. J Biomed Biotechnol 20122012: 460841.
[46] Akhoondinasab MR, Khodarahmi A, Akhoondinasab M, Saberi M, Iranpour M. Assessing effect of three herbal medicines in second and third degree burns in rats and comparison with silver sulfadiazine ointment. Burns 2015;41:125–31.
[47] Al-Amoudi A, Dubochet J, Norlen L. Nanostructure of the epidermal extracellular space as observed by cryo-electron microscopy of vitreous sections of human skin. J Invest Dermatol 2005;124:764–77.